Human Pathology (2019) **90**, 45–53

ELSEVIER

Human PATHOLOGY

www.elsevier.com/locate/humpath

Original contribution

EWSR1/FUS-NFATc2 rearranged round cell sarcoma: clinicopathological series of 4 cases and literature review☆

Julio A. Diaz-Perez[a], G. Petur Nielsen[b], Cristina Antonescu[c], Martin S. Taylor[b], Santiago A. Lozano-Calderon[d], Andrew E. Rosenberg[a,*]

[a]*Department of Pathology and Laboratory Medicine, Miller School of Medicine, University of Miami, Miami, FL*
[b]*Department of Pathology and Laboratory Medicine, Massachusetts General Hospital, Harvard University, Boston, MA*
[c]*Department of Pathology, Memorial Sloan Kettering Cancer Center, New York, NY*
[d]*Department of Orthopedics, Massachusetts General Hospital, Harvard University, Boston, MA*

Received 29 March 2019; accepted 5 May 2019

Keywords:
NFATc2-EWSR1;
FUS;
Ewing sarcoma;
Bone neoplasms;
Round cell sarcoma;
Undifferentiated sarcoma

Summary The classification of bone neoplasms composed of small round cells is experiencing a transformation after the discovery of various gene fusion rearrangements that determine diagnosis, behavior, and response to therapy. We present herein 4 new cases of small round cell tumor of the bone that harbor *NFATc2* rearrangements involving either *EWSR1* or *FUS* genes. We studied the clinical presentation, pathologic features, genetics (FISH, targeted RNA sequencing) and outcome in these 4 patients. We also reviewed the literature describing similar cases. All our patients were male. The median age at diagnosis was 33.5 years. All tumors presented in long bones of the extremities as a large destructive mass with a mean size of 12.5 cm. All cases were hypercellular with prominent collagenous stroma and consisted of small to medium size round cells arranged in cords, thin trabeculae, and pseudoacinar structures. Most cases showed focal or diffuse membrane staining for CD99; whereas S100, synaptophysin and chromogranin were negative. EMA showed cytoplasmic staining in one case. Genetic studies identified *EWSR1-NFATc2* fusion in 3 cases, and *FUS-NFATc2* fusion in one case. Two patients were treated with neoadjuvant chemotherapy using Ewing sarcoma regimens, and surgical excision was performed on 3 patients; necrosis was minimal. Follow-up is limited; after a median follow-up of 8.7 months, one patient developed local recurrence and metastases to the lungs. Poorly differentiated round cell sarcoma with *EWSR1/FUS-NFATc2* fusions are uncommon. The tumors have consistent clinical findings, morphology, and immunoprofile that in combination are distinctive and differ from that of Ewing sarcoma. Importantly, these tumors do not respond to Ewing sarcoma chemotherapy regimens.

1. Introduction

Malignant small round cell tumors of bone encompass a heterogeneous group of neoplasms most commonly diagnosed in children and young adults. These neoplasms are

☆ The authors do not have conflict of interest to declare.

* Corresponding author at: University of Miami Hospital, 1400 NW 12th Avenue, Room 4060 Miami, FL 33136.
E-mail address: ARosenberg@med.miami.edu (A. E. Rosenberg).

https://doi.org/10.1016/j.humpath.2019.05.001
0046-8177/

highly aggressive and often associated with the development of disseminated disease [1,2]. During the last 2 decades, specific molecular alterations identified in these neoplasms have allowed the creation of a new classification scheme that may bring therapeutic benefit. Currently, the largest group of small round cell tumors of bone is Ewing sarcoma that is characterized by specific translocation fusion genes *EWSR1/FUS-ETS.* [1,3]. Other tumors with similar but more variable morphology and behavior have been grouped in the so-called 'Ewing-like' tumors; they possess specific fusions such as *CIC-DUX4, BCOR-CCNB3,* and *EWSR1-NFATc2* [2-4]. To date, the information known about NFATc2 rearranged bone tumors is limited to mainly single case reports and sporadic descriptions within Ewing family series of tumors many of them without clinicopathological information [5,6]. Herein we describe the clinicopathological features of 4 new cases of malignant small round cell sarcoma of bone that harbor *EWSR1/FUS-NFATc2* translocation gene fusions.

2. Materials and methods

Cases were identified from the surgical pathology databases of the consultations of one of the authors (AER), and Massachusetts General Hospital between January 2016 and December 2018. Relevant clinical data was collected including gender, age at diagnosis, location and size of tumor, imaging features, treatment, and follow-up.

All tumors were routinely fixed and processed, embedded in paraffin, and stained with hematoxylin and eosin. Formalin-fixed, paraffin-embedded (FFPE) sections of 4-μm thickness were stained with the immunohistochemistry antibodies presented in Table 1 according to standard technique.

2.1. Fluorescence in situ hybridization

The *EWSR1-NFATc2* fusion was investigated by a dual-color FISH assay on interphase nuclei from paraffin-embedded 4-μm-thick sections with Spectrum Green-labeled BAC clones RP11-367E7 and RP11-480 L23 corresponding to the *EWSR1*-5 region and Spectrum Red-labeled BAC clones RP11-2 L23 and RP11-73P15 corresponding to the *NFATC2*-3′ region (Empire Genomics, Buffalo, NY) [7,8].

2.2. RNA extraction and sequencing

An RT-PCR assay for the EWSR1-NFATC2 fusion transcript was performed with an *EWSR1* exon 8 forward primer (TGGGTGTTTATGGGCAGGAGTC) and an *NFATC2* exon 5 reverse primer (GCTCAATGTCGGCGTTTCTAAG) to amplify a 573 base pair product. As a control assay, the wild-type FOXO1 transcript was assayed by RT-PCR with an *FOXO1* exon 1 forward primer (GCAGATCTACGAGTGGATGG) and an *FOXO1* exon 2 reverse primer (AACTGTGATCCAGGGCTGTC) to amplify a 323 base pair product. The RT-PCR was performed with the SuperScript III One-Step RT-PCR System with Platinum Taq DNA Polymerase (Life Technologies, Carlsbad, CA).

Next generation sequencing studies were conducted from libraries prepared from nucleic acid extracted from unstained slides or paraffin blocks from the best tumoral area. For the 3 samples from the consultation files, these were conducted following the FoundationOne protocol (Foundation Medicine, Inc. Cambridge, MA). For the one sample from Massachusetts General Hospital, the clinically validated Solid Fusion and Sarcoma Fusion Assays used Anchored Multiplex PCR with a custom ArcherDx library (ArcherDx, Boulder, CO) followed by a laboratory-developed algorithm to detect and annotate fusion

Table 1 Antibodies used in the immunophenotypic study of our cases

Antibody	Clone	Manufacturer	Control	Antigen retrieval	Dilution	Temperature (°C)
CD99	EPR3097Y	Cell Marque	Pancreas	High pH ER2 for 30 min	RTU	100
Pan CK	AE1/AE3	Leica	Liver	Enzyme 1 for 5 min	RTU	100
Syn	27G12	Leica	Pancreas	Er2 for 15 min	RTU	100
Chr	5H7	Leica	Pancreas	Low pH ER1 for 15 min	RTU	100
S100	Polyclonal	Leica	Nerve	Enzyme 1 for 10 min	1:800	100
EMA	E29	Cell Marque	Breast	Er2 for 15 min	RTU	100
p63	4A4	Biocare	Prostate	Er2 for 30 min	RTU	100
Desmin	DE-R-11	Leica	Colon	Er2 for 20 min	RTU	100
SMA	ASM-1	Leica	Skin	None	RTU	100
WT1	WT49	Leica	Fallopian Tube	Er2 for 30 min	RTU	100
ERG	EP111	Dako	Spleen	Er2 for 40 min	RTU	99
CD34	QBEND/10	Leica	Tonsil	Er2 for 5 min	RTU	100
SATB2	EP281	Cell Marque	Colon	Er2 for 20 min	RTU	100
INI-1	MRQ-27	Cell Marque	Colon	Er2 for 40 min	RTU	100
Ki-67	K2	Leica	Tonsil	E2 [20]	RTU	100

Abbreviations: Pan CK, pancytokeratin; Syn, Synaptophysin; Chr, Chromogranin EMA, epithelial membrane antigen; SMA, smooth muscle actin; WT1, Wilms tumor 1; ;RTU, ready to use.

Table 2 Clinical features of previously published and current report cases of *EWSR1/FUS-NFATc2* positive malignant round cell sarcomas.

Case #	First Author	Year	Age (y)	Gender	Body site	Size (cm)	CT or RT/response	Follow-up
1	Szuhai et al [14]	2009	39	Male	Humerus	N/A	N/A	N/A
2	Szuhai et al [14]	2009	16	Male	Femur	N/A	N/A	N/A
3	Szuhai et al [14]	2009	21	Male	Thigh soft tissue	N/A	N/A	N/A
4	Szuhai et al [14]	2009	25	Male	Femur	N/A	N/A	N/A
5-6	Wang et al [15]	2012	N/A	N/A	N/A	N/A	N/A	N/A
7	Romeo et al [18]	2012	32	Male	Lower extremity	N/A	N/A	NED, 64 m
8	Sadri et al [19]	2014	30	Male	Femur	8.3	N/A	LR, 30 m
9	Kinkor et al [20]	2014	12	Male	Femur	7	CT/No response	NED, 11 m
10	Kinkor et al [20]	2014	28	Male	Femur	2	RT and CT/No response	LR and lung metastases, 48 m
11 [a]	Brohl et al [28]	2014	15	Male	Femur	N/A	N/A	N/A
12-17	Charville et al [25]	2017	N/A	N/A	N/A	N/A	N/A	N/A
18	Cohen et al [6]	2018	24	Female	Calf soft tissue	6	CT/No response	NED, 12 m
19-26	Baldauf et al [5]	2017	N/A	N/A	N/A	N/A	N/A	N/A
27	Toki et al [22]	2018	N/A	N/A	N/A	N/A	N/A	N/A
28	Watson et al [16]	2018	32.7	Male	Humerus	N/A	N/A	N/A
29	Watson et al [16]	2018	12.7	Female	Tibia	N/A	N/A	N/A
30	Watson et al [16]	2018	61.5	Male	Calf soft tissue	N/A	N/A	N/A
31	Watson et al [16]	2018	23.6	Male	Femur	N/A	N/A	N/A
32 [a]	Watson et al [16]	2018	33.3	Male	Femur	N/A	N/A	N/A
33 [a]	Watson et al [16]	2018	49	Female	Femur	N/A	N/A	N/A
34 [a]	Watson et al [16]	2018	43.3	Male	Femur	N/A	N/A	N/A
35	Yau et al [21]	2019	43	Male	Femur	8.5	RT and CT/No response	NED, 12 m
36	Bode- Lesniewska et al [17]	2019	34	Female	Femur	N/A	CT	Metastasis: Skin, 54 m, lung 132 m
37	Bode- Lesniewska et al [17]	2019	42	Male	Tibia	N/A	N/A	NED, 102 m
38	Bode- Lesniewska et al [17]	2019	60	Female	Abdomen	N/A	N/A	NED, 8 m
39 [a]	Bode- Lesniewska et al [17]	2019	12	Male	Humerus	N/A	N/A	NED, 8 m
40	Wang et al [38]	2019	67	Male	Radius	N/A	RT and CT/10% tumor necrosis	NED, 14 m
41	Wang et al [38]	2019	32	Male	Periclavicular soft tissue	N/A	RT and CT/90% tumor necrosis	NED, 24 m
42	Wang et al [38]	2019	42	Male	Radius	N/A	RT and CT/No response	AWD, 16 m
43	Wang et al [38]	2019	24	Female	Calf soft tissue	N/A	RT and CT/10% tumor necrosis	NED, 23 m
44	Wang et al [38]	2019	42	Male	Radius	N/A	N/A	Soft tissue and bone metastases, DOD, 93 m
45	Wang et al [38]	2019	59	Male	Periclavicular soft tissue	N/A	RT and CT/No response	LR, NED, 144 m
46	Current report	2019	28	Male	Tibia	4.2	RT and CT/No response	NED, 8.7 m
47	Current report	2019	39	Male	Femur	14.5	RT and CT/No response	NED, 30 m
48 [a]	Current report	2019	28	Male	Humerus	18	RT and CT	Preparing for resection
49	Current report	2019	46	Male	Femur	13.4	RT and CT/No response	LR and lung metastases, 5.9 m later

Abbreviations: m: months; cm: centimeters; ;N/A, not available, NED, no evidence of disease; LR, local recurrence; CT, chemotherapy; RT, radiotherapy; AWD, alive with disease; DOD, death of disease.

[a] *FUS-NFATc2* case.

transcripts [7]. Sequencing was performed on either a MiSeq, HiSeq 4000, or NextSeq instrument (Illumina®, San Diego CA).

3. Results

The clinical characteristics of the 45 cases previously published and our current 4 cases (cases 46-49) are presented in Table 2. In our series all patients were male. The median age at diagnosis was 33.5 (range, 28-46) years. One case was noted for "many" years, one patient had pain for 1 year, one patient had pain for 3 months and the last patient experienced pain for 1 month. There was no previous history of trauma. All tumors arose in long bones and ranged in size from 4.2 to 18 (mean size 12.5) cm. The tumor that was noted for years was located on the surface of the femur and eroded into the medullary canal and the other 3 tumors manifest as poorly defined, lytic tumors that originated within the medullary cavity, destroyed the cortex, and extended into the soft tissues (Fig. 1). Staging studies revealed that the tumors were non-metastatic at the time of diagnosis.

Grossly, the tumors were solid, pink-tan, and fish flesh-like in appearance, and involved the medullary cavity and soft tissues (Fig. 2). Histologically, the initial diagnosis was myoepithelial carcinoma (n = 2), and Ewing-like sarcoma (n = 2). The histomorphologic features were distinctive (Cases 46 to 49, table 3). All of the tumors grew with an infiltrative pattern and replaced the marrow, encased preexisting bony trabeculae, and percolated within Haversian systems (Fig. 3). The tumor cells were small to medium size, round or short spindle in shape, and were arranged in small, round to oval, sometimes pseudoacinar groups delineated by a collagenous stroma. Other patterns included trabeculae or cords of cells demarcated by collagen fibers. The nuclei ranged from hyperchromatic to having fine chromatin, absent or conspicuous nucleoli, with irregular or smooth nuclear membranes and the cytoplasm was eosinophilic or clear. Mitoses were infrequent in most cases; however, one case had 34 mitoses per 10 high-power fields. A focal branching staghorn-like vascular pattern was present in all tumors. Scattered small foci of necrosis were present in 3 cases. In the tumor arising on the surface of the bone a component of the neoplasm was less cellular and composed of bland spindle cells arranged in a myxocollagneous stroma with no mitotic activity.

3.1. Immunohistochemistry

Results are summarized in Table 3. Most of our tumors (cases 46 to 49) showed focal or diffuse membrane staining for CD99; whereas S100, synaptophysin and chromogranin were negative in all cases. EMA and p63 focal staining was documented in one case (case 42). The tumor cells were negative for pan keratin, SMA, desmin, WT1, ERG, and CD34. SATB2 was positive in 2 of 3 cases tested. INI-1 (BAF47) nuclear staining was retained in 2 cases tested.

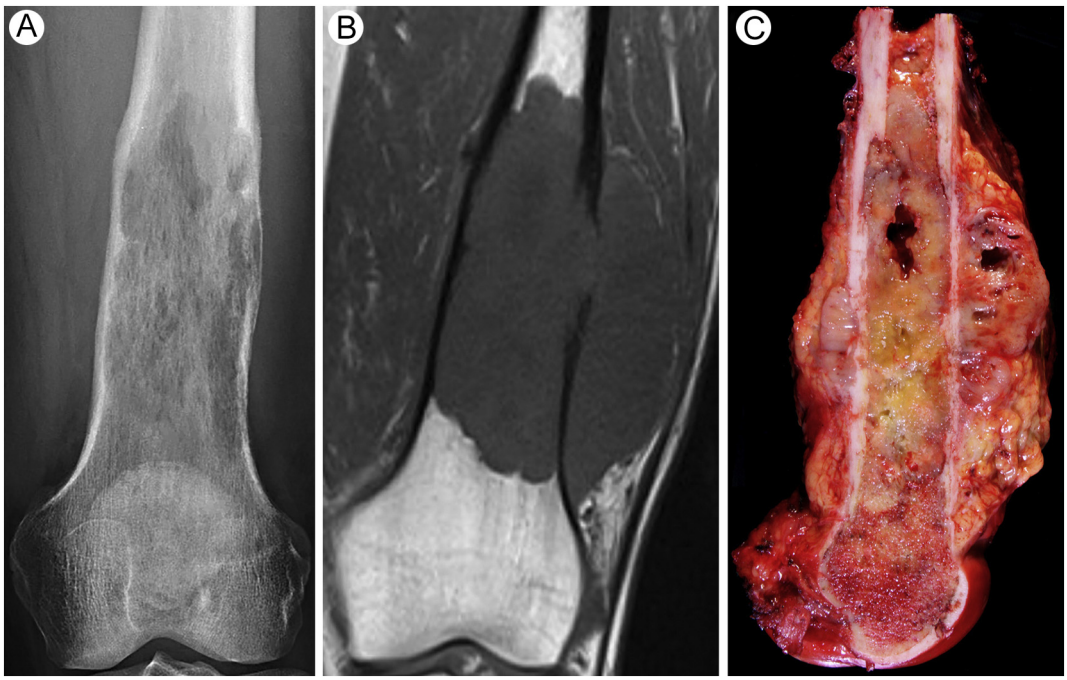

Figure 1 The tumor is lytic and poorly defined (A), has low signal intensity on T1-weighted images and extends into soft tissue (B). The tumor is centered in the medullary cavity and is soft pink-tan in appearance. Note the soft tissue component (C).

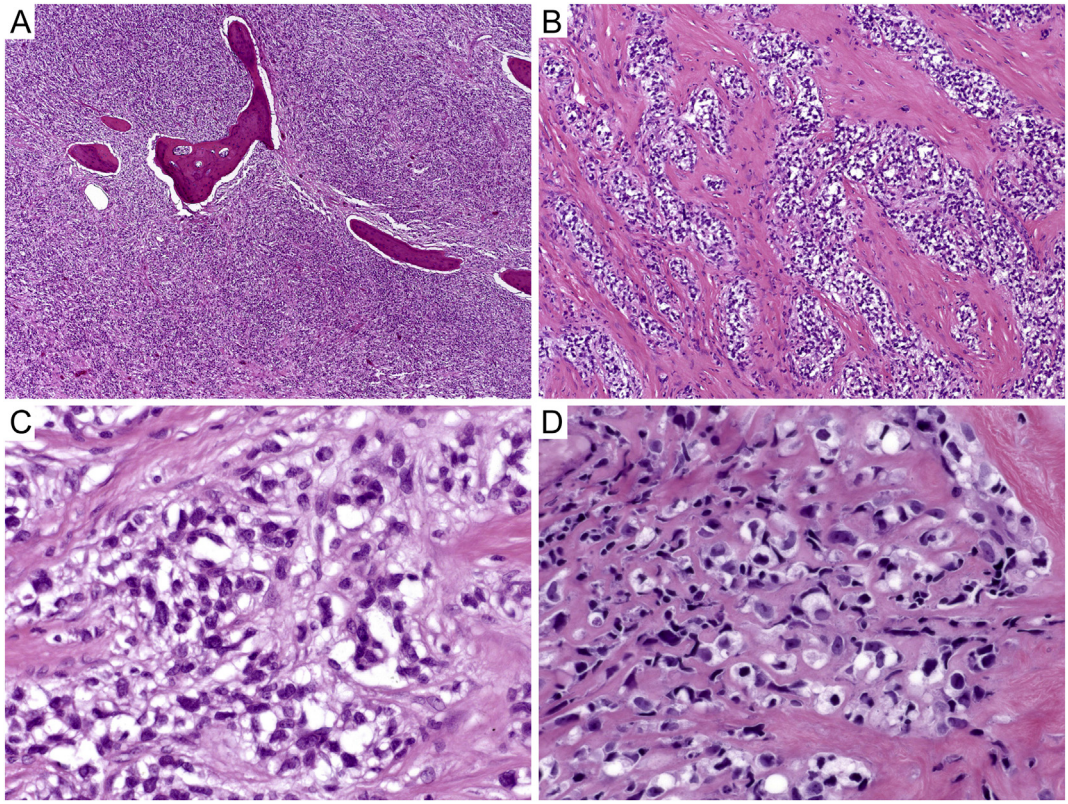

Figure 2 Microscopically, the tumors were hypercellular with prominent eosinophilic collagenous stroma and grew with an infiltrative pattern encasing preexisting bony trabeculae (A; HE original magnification ×2). Tumor cells were arranged in cords, trabeculae and formed pseudoacinar structures (B; HE, original magnification ×4), and were delineated by collage fibers (C; HE, original magnification ×20). Nuclear irregularity with inconspicuous nucleoli and eosinophilic or clear cytoplasm was present (D; HE, original magnification ×40).

3.2. Molecular studies

Three cases were tested by FISH and confirmed to have *EWSR1* gene rearrangements in 2 cases and FUS gene rearrangement in one case (Table 4). All 3 cases were also confirmed to have an *NFATc2* break-apart rearrangement. In one case the rearrangement was associated with amplification of the *EWSR1-NFATc2* fusion signals as previously described [14]. The case harboring an *FUS-NFATc2* fusion showed a polyploidy signal below the level of amplification, while the remaining *EWSR1-NFATc2* case showed no copy gains. Targeting RNA sequencing identified *EWSR1-NFATc2* fusion in 2 cases and *FUS-NFATc2* fusion gene in one case. Other additional genetic abnormalities in single cases were identified, including gene fusions, such as *ACTN2-ALK*, *KDM6A* loss of exons 3-5, *TP53-SAB1*, and *FOXO1-NKAIN2*, of uncertain functional significance.

Three of our four patients were treated with neo-adjuvant therapy using Ewing sarcoma regimens, and one (case 4) was treated post-operatively with cisplatin and adriamycin. Three tumors underwent limb salvage resection with negative margins. One patient is recent, and the patient is being prepared for resection. Tumor response, in the two treated patients, represented by necrosis was poor and less than 20% in the resection specimens. Post-surgical follow-up ranged from 5.9 to 30 (median, 8.7) months. One patient developed metastases to the lung and experienced local recurrence after 5.9 m of follow-up. No patient has died from disease.

4. Discussion

Studies of fusion genes in small round cell sarcomas have resulted in the discovery of new genetic abnormalities that help define distinct entities. The flag bearer of this group of tumors is Ewing sarcoma which harbors rearrangement of *EWSR1*; however, this genetic abnormality is also present in other tumor types including Ewing-like sarcoma defined by *EWSR1* fusions with non-TET/ETS gene partners, myoepithelial carcinoma, extraskeletal myxoid chondrosarcoma, clear cell sarcoma, and desmoplastic small round cell tumor, amongst others [1,2]. In this study we describe the features of tumors with *EWSR1* or *FUS - NFATc2* fusions.

NFATc2 function is controlled by calcium-dependent activity of calcineurin, which dephosphorylates inhibitory phosphate residues. This action exposes a nuclear localization signal, thus allowing NFATc2 to traffic into the nucleus where it interacts with the transcription factor AP1,

Table 3 Histopathology and immunophenotype of previously published and current report cases of *EWSR1/FUS-NFATc2* rearranged malignant round cell sarcomas.

Case #	Cell morphology	Pattern	Stroma	Mitosis/necrosis	CD99	EMA	Keratin	Desmin	S100
1	Small round cells	Cords, solid	Fibrous	N/A	+	N/A	–	–	–
2	Small round cells	Cords, solid	Fibrous	N/A	+	N/A	–	–	–
3	Small round cells	Nets	Fibrous	N/A	+	N/A	–	–	–
4	Small round cells	Cords, solid	Fibrous	N/A	+	N/A	–	N/A	–
5,6	N/A	N/A	N/A	N/A	N/A	N/A	N/A	N/A	N/A
7	Epithelioid and spindle cells	Sheets	Minimal	N/A	+	+	Dot-like +	–	–
8	Epithelioid clear cells	Sheets	Fibrous	8 per HPF/Present	+	–	Dot-like +	N/A	–
9	Epithelioid clear cells	Nets	Fibrous	Few/None	+	–	–	N/A	–
10	Small round cells	Cords and trabeculae	Fibromyxoid	Few/None	+	–	–	–	–
11 [a]	N/A	N/A	N/A	N/A	N/A	N/A	N/A	N/A	N/A
12-17	N/A	N/A	N/A	N/A	N/A	N/A	N/A	N/A	N/A
18	Small round cells	Cords and trabeculae	Fibromyxoid	None/None	+	Dot-like +	Dot-like +	–	–
19-26	N/A	N/A	N/A	N/A	N/A	N/A	N/A	N/A	N/A
27	N/A	N/A	N/A	N/A	N/A	N/A	N/A	N/A	N/A
28-31	N/A	N/A	N/A	N/A	N/A	N/A	N/A	N/A	N/A
32-34 [a]	N/A	N/A	N/A	N/A	N/A	N/A	N/A	N/A	N/A
35	Small round cells	Sheets	Minimal	>30 per 10 HPF/Present	+	N/A	Dot-like +	N/A	N/A
36	Small round cells	Trabeculae	Fibrous	N/A	+	N/A	–	–	–
37	Small round cells	Nets and trabeculae	Fibrous	N/A	+	+	N/A	–	–
38	Small round cells	Trabeculae	Fibrous	N/A	+	Focal +	Focal +	–	–
39 [a]	Spindle cells	Trabeculae	Fibrous	None	+	+	–	–	–
40	N/A	N/A	N/A	N/A	+	Focal +	Focal dot	N/A	N/A
41	N/A	N/A	N/A	N/A	+	+	N/A	N/A	N/A
42	N/A	N/A	N/A	N/A	+	Focal +	N/A	N/A	N/A
43	N/A	N/A	N/A	N/A	+	N/A	Focal dot	N/A	N/A
44	N/A	N/A	N/A	N/A	+	+	Focal dot	N/A	N/A
45	N/A	N/A	N/A	N/A	+	+	N/A	N/A	N/A
46	Small round cells	Nets and cords	Fibrous	<5 per 10 HPF/None	+	–	–	–	–
47	Epithelioid and spindle cells	Nets and cords	Fibrous	<5 per 10 HPF/None	+	Focal +	–	N/A	–
48 [a]	Epithelioid and spindle cells	Nets and cords	Fibrous	<5 per 10 HPF/ Present	+	N/A	–	–	–
49	Epithelioid and spindle cells	Nests, cords and solid areas	Fibrous	34 per 10 HPF/ Present	–	–	–	–	–

Abbreviations: CK, pancytokeratin; EMA, epithelial membrane antigen; Des, desmin; HPF, high-power fields, and N/A, not available.
[a] *FUS-NFATc2* case.

composed of fos and jun proteins. The *EWSR1-NFATc2* fusion that corresponds to t(20;22) (q13.2;q12.2) results in a truncated *NFATc2* protein with loss of the first 2 exons, which encode the regulatory region. In the absence of negative phosphorylation signals, *NFATc2* is thought to freely and constitutively translocate to the nucleus targeting genes in homology to the NF-kappa B proteins [8,9]. *NFATc2* is involved in chondrogenesis, T-cell differentiation and transcriptional activation of cytokine genes, osteoclast differentiation, cardiac valve morphogenesis, and regulates myosin heavy chain gene expression in skeletal muscle [8-10].

EWSR1 and *FUS* are both within the *FUS* family of proteins. Oncogenic fusions of both proteins typically combine the N-terminal transcriptional activation domain (TAD) of *EWSR1/FUS* with the DNA binding domain (DBD) of a fusion partner such as *NFATc2*, as in our 4 cases. The *EWSR1/FUS* TADs are unstructured sequences that are thought to activate transcription at sites of DBD chromatin binding through the process of phase-separation, forming local liquid-like condensates along with the Mediator coactivator at sites of transcriptional activation [11,12]. A previous study established that the breakpoint is located in the

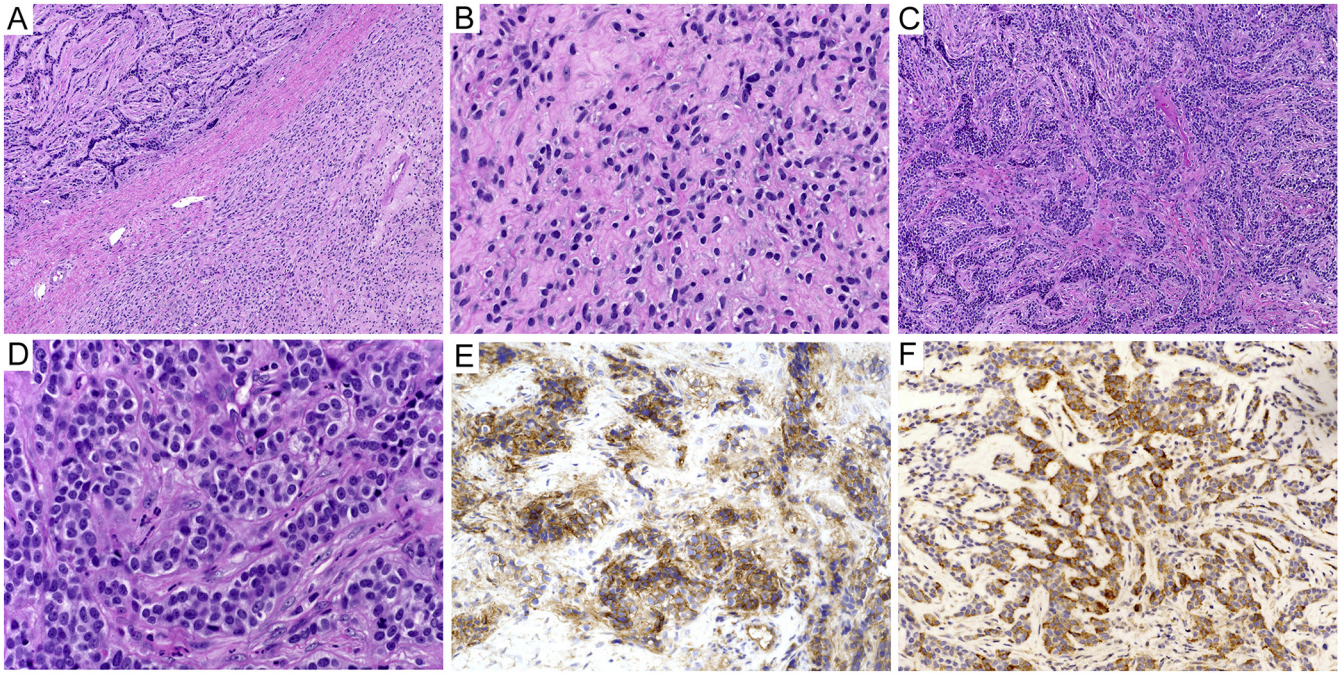

Figure 3 One of our tumors (case 13 in the summary table) had 2 components (A; HE, original magnification ×2). One area was hypocellular and the tumor cells showed banal morphology (B; HE, original magnification ×20), and the other region was hypercellular with the tumor cells arranged in elongate nests (C; HE, original magnification ×10 and D; HE, original magnification ×20). The tumor cells were positive for CD99 (E, original magnification ×20), and case 13 was also positive for EMA (F, original magnification ×10).

NFATc2 gene 5′ region in intron 2 and intron 3, allowing for a junction between the 3′ end of exon 8 of *EWSR1* and the 5′ end of *NFATc2* exon 3. The resulting fusion protein lacks the COOH-terminal RNA binding domain of *EWSR1* and the NH2-terminal transactivation domain and regulatory domain of *NFATc2* [13].

Szuhai et al in 2009 reported the presence of *NFATc2* fusions in 4 cases of Ewing sarcoma [13]. Subsequently, investigators have postulated that round cell tumors with this gene fusion should constitute a distinct clinicopathological entity [6]. To date, 45 cases have been documented in the literature of which 24 cases (53.3%) have clinicopathological information provided (Tables 2 and 3). Some large series of Ewing sarcoma have described the genetic profile of *EWSR1/FUS-NFATc2* tumors but do not include clinical and/or pathologic features [14,15]. Of the cases with known clinical information including our 4 cases, the patients have ranged in age from 12 to 67 years, median 32.3 years, and have male predominance with a M:F ratio of 5:1. The tumors have arisen in long bones of the extremity; 14 cases in the femur, 4 in the humerus, 3 in the tibia, and 3 in the radius. Only 7 cases of probable soft tissue origin have been documented (Cases #3, 18, 30, 38, 41, 43, and 45). Interestingly, the patients in several cases had symptoms for years prior to diagnosis and in one of our cases the tumor had a component that suggested a benign precursor that at the time was interpreted as representing a benign myoepithelioma that underwent malignant transformation. Neo-adjuvant therapy using Ewing regimens was reported in 14 cases and most had poor responses in terms of percent necrosis. Twenty-three of 24 patients underwent surgical excision. Of 19 patients with follow-up, 4 (21%) experienced local recurrence and 4 (21%) developed lung, cutaneous, or bone metastases after a median follow up of 23 months, range 5.9 to 144 (Table 2). Fatal outcomes have not been reported. Hopefully, these tumors will benefit from new targeted therapeutic

Table 4 Genetic alterations in our tumors.

Case #	FISH	*EWSR1/FUS* fusion	Additional fusions
13	*EWSR1* rearrangement	*EWSR1-NFATc2*	*ACTN2-ALK*
14	*EWSR1-NFATc2*	*EWSR1-NFATc2*	None
15 [a]	*FUS- NFATc2*	*FUS-NFATc2*	*KDM6A* loss exons 3-5, *TP53-SAB1*
16	*EWSR1-NFATc2*	*EWSR1-NFATc2*	*FOXO1-NKAIN2*

Abbreviations: FISH, fluorescent in situ hybridization.
[a] FUS-NFATc2 case.

regimens; in vitro studies have shown that therapy against NFATc2/calcineurin and EZH2 may be of utility [28,29].

The phenotype of *EWSR1/FUS-NFATc2* tumors is under study. Originally, some hypothesized it may be a type of myoepithelial carcinoma because of the morphology, rearrangement of EWSR1, and expression of epithelial markers — cytokeratin or EMA expression have been documented in 14 of 24 cases tested (58.3%) (Cases 7, 8, 13, 30, 32, 33, 34, 36, 40-45); however, this classification has not been confirmed or excluded. The one patient of ours that had a benign appearing precursor that resembles myoepithelioma supports this hypothesis. *EWSR1/FUS-NFATc2* tumors share similar immunophenotype with other *EWSR1-FLI1* and *EWSR1-ERG* tumors, almost all cases (95.8%) known have shown expression of CD99, also they are positive for PAX7 and NKX2.2 [6,21–25]. Recently, Koelsche et al [26] reported that *EWSR1-NFATc2* fusion small round cell sarcoma has a unique methylation pattern that segregates it from other members of the Ewing sarcoma family.

One tumor in our series had a *FUS-NFATc2* fusion, a finding previously reported by Brohl and Watson in a large series describing the genomic landscape of Ewing Sarcoma [15,27]. However, no clinicopathological information was made available until recently (cases highlighted on gray, Tables 2 and 3) [16]. *FUS* is well known to substitute for *EWSR1* in translocation fusion genes. All additional genetic lesions we report in our cases are felt to be secondary to the *EWSR1/FUS-NFATc2* rearrangement and likely represent genetic instability in these tumors [28]. *KDM6A* loss of exons 3-5 and a *TP53-SAB1* fusion were identified in one case—these aberrations are known to be associated with drug resistance and high proliferation [29-32]. The *ACTN2-ALK* fusion of actinin-2 (*ACTN2*) to the anaplastic lymphoma kinase (*ALK*) has not been reported, nor has an *ALK* fusion in a Ewing or Ewing-like sarcoma. We speculate that this is likely active but of unclear clinical significance, as *ACTN2* has a strong N-terminal homodimerization domain, the prerequisite for *ALK* activation by fusion [33], and additionally ALK has been reported to be expressed in a high percentage of Ewing Sarcomas [34]. Regarding the candidate *FOXO1-NKAIN2* fusion, NKAIN2 is a poorly characterized candidate tumor suppressor gene; fusions and translocations that have been previously reported for this protein are typically either inactivating or out-of-frame [35]. *FOXO1* fusions to *PAX3* or *PAX7* include the *FOXO1* C-terminal transcriptional activation domain (TAD), aberrantly activating PAX3/7 targets [36]. Given the lack of the *FOXO1* TAD in this N-terminal FOXO1 fusion, it is difficult to imagine a similar function for this fusion, and we therefore speculate that this is a passenger aberration.

In conclusion, *EWSR1/FUS-NFATc2* fusion positive round cell sarcomas are uncommon, have distinct morphology, and are potentially biologically aggressive. They are important to recognize because they respond poorly to Ewing sarcoma regimens and new forms of therapy are needed.

Acknowledgements

We thank Dr. Katie Dennis and Dr. Howard Rosenthal from the University of Kansas, Dr. Mashe Fried from The Rofeh Cholim Cancer Society, and Dr. Douglas O. Reale from the Baptist Hospital of Miami for providing the cases and clinical information. This project was supported by grants P50 CA217694 (CRA), and P30 CA008748 (CRA).

References

[1] Thway K, Fisher C. Mesenchymal tumors with EWSR1 gene rearrangements. Surg Pathol Clin 2019 Mar;12(1):165-90.
[2] Grünewald TGP, Cidre-Aranaz F, Surdez D, et al. Ewing sarcoma. Nat Rev Dis Primers 2018 Jul 5;4(1):5.
[3] Miettinen M, Felisiak-Golabek A, Contreras AL, et al. New fusion sarcomas histopathology and clinical significance of selected entities. Hum Pathol 2019 Apr;34:86-65.
[4] Machado I, Yoshida A, Morales MGN, et al. Review with novel markers facilitates precise categorization of 41 cases of diagnostically challenging, "undifferentiated small round cell tumors". A clinicopathologic, immunophenotypic and molecular analysis. Ann Diagn Pathol 2018 Jun;34:1-12.
[5] Baldauf MC, Orth MF, Dallmayer M, et al. Robust diagnosis of Ewing sarcoma by immunohistochemical detection of super-enhancer-driven EWSR1-ETS targets. Oncotarget 2017 Aug 4;9(2):1587-601.
[6] Cohen JN, Sabnis AJ, Krings G, Cho SJ, Horvai AE, Davis JL. EWSR1-NFATC2 gene fusion in a soft tissue tumor with epithelioid round cell morphology and abundant stroma: a case report and review of the literature. Hum Pathol 2018 Nov;81:281-90.
[7] Jo VY, Antonescu CR, Zhang L, Dal Cin P, Hornick JL, Fletcher CD. Cutaneous syncytial myoepithelioma: clinicopathologic characterization in a series of 38 cases. Am J Surg Pathol 2013 May;37(5):710-8.
[8] Li C, Zheng Z, Zhang X, Asatrian G, Chen E, Song R, Culiat C, Ting K, Soo C. Nfatc1 Is a Functional Transcriptional Factor Mediating Nell-1-Induced Runx3 Upregulation in Chondrocytes. Int J Mol Sci. 2018 Jan 6; 19(1). pii: E168.
[9] Perotti V, Baldassari P, Molla A, et al. An actionable axis linking NFATc2 to EZH2 controls the EMT-like program of melanoma cells. Oncogene 2019 Feb;1.
[10] Ranger AM, Gerstenfeld LC, Wang J, et al. The nuclear factor of activated T cells (NFAT) transcription factor NFATp (NFATc2) is a repressor of chondrogenesis. J Exp Med 2000 Jan 3;191(1):9-22.
[11] Wang J, Choi JM, Holehouse AS, et al. A molecular grammar governing the driving forces for phase separation of prion-like RNA binding proteins. Cell 2018 Jul 26;174(3):688-699.e16.
[12] Boija A, Klein IA, Sabari BR, et al. Transcription factors activate genes through the phase-separation capacity of their activation domains. Cell 2018 Dec 13;175(7):1842-1855.e16.
[13] Szuhai K, Ijszenga M, de Jong D, Karseladze A, Tanke HJ, Hogendoorn PC. The NFATc2 gene is involved in a novel cloned translocation in a Ewing sarcoma variant that couples its function in immunology to oncology. Clin Cancer Res 2009 Apr 1;15(7):2259-68.
[14] Wang WL, Patel NR, Caragea M, et al. Expression of ERG, an Ets family transcription factor, identifies ERG-rearranged Ewing sarcoma. Mod Pathol 2012 Oct;25(10):1378-83.
[15] Watson S, Perrin V, Guillemot D, et al. Transcriptomic definition of molecular subgroups of small round cell sarcomas. J Pathol 2018 May;245(1): 29-40.
[16] Bode-Lesniewska B, Fritz C, Ulrich Exner G, Wagner U, Fuchs B. EWSR1-NFATC2 and FUS-NFATC2 gene fusion-associated mesenchymal tumors: Clinicopathologic correlation and literature review. Sarcoma 2019;9386390.

[17] Romeo S, Bovée JV, Kroon HM, et al. Malignant fibrous histiocytoma and fibrosarcoma of bone: a re-assessment in the light of currently employed morphological, immunohistochemical and molecular approaches. Virchows Arch 2012 Nov;461(5):561-70.
[18] Sadri N, Barroeta J, Pack SD, et al. Malignant round cell tumor of bone with EWSR1-NFATC2 gene fusion. Virchows Arch 2014 Aug;465(2):233-9.
[19] Kinkor Z, Vaneček T, Svajdler Jr M, et al. Where does Ewing sarcoma end and begin—two cases of unusual bone tumors with t(20;22)(EWSR1-NFATc2) alteration. Cesk Patol 2014 Apr;50(2):87-91.
[20] Yau DTW, Chan JKC, Bao S, Zheng Z, Lau GTC, Chan ACL. Bone sarcoma with EWSR1-NFATC2 fusion: sarcoma with varied morphology and amplification of fusion gene distinct from Ewing sarcoma. Int J Surg Pathol 2019 Feb 3:1066896919827093.
[21] Toki S, Wakai S, Sekimizu M, et al. PAX7 immunohistochemical evaluation of Ewing sarcoma and other small round cell tumours. Histopathology 2018 Oct;73(4):645-52.
[22] Charville GW, Wang WL, Ingram DR, Roy A, Thomas D, Patel RM, Hornick JL, van de Rijn M, Lazar AJ. Malignant fibrous histiocytoma and fibrosarcoma of bone: a re-assessment in the light of currently employed morphological, immunohistochemical and molecular approaches. PAX7 expression in sarcomas bearing the EWSR1-NFATC2 translocation. Mod Pathol 2019 Jan;32(1):154–156.
[23] Hung YP, Fletcher CD, Hornick JL. Evaluation of NKX2-2 expression in round cell sarcomas and other tumors with EWSR1 rearrangement: imperfect specificity for Ewing sarcoma. Mod Pathol 2016 Apr;29(4):370-80.
[24] Charville GW, Wang WL, Ingram DR, et al. EWSR1 fusion proteins mediate PAX7 expression in Ewing sarcoma. Mod Pathol 2017 Sep;30(9):1312-20.
[25] Toki S, Wakai S, Sekimizu M, et al. PAX7 immunohistochemical evaluation of Ewing sarcoma and other small round cell tumours. Histopathology 2018 Oct;73(4):645-52.
[26] Fernandez-Pol S, van de Rijn M, Natkunam Y, Charville GW. Immunohistochemistry for PAX7 is a useful confirmatory marker for Ewing sarcoma in decalcified bone marrow core biopsy specimens. Virchows Arch 2018;473(6):765-9.
[27] Brohl AS, Solomon DA, Chang W, et al. The genomic landscape of the Ewing sarcoma family of tumors reveals recurrent STAG2 mutation. PLoS Genet 2014 Jul 10;10(7):e1004475.
[28] Lang T, Ding X, Kong L, et al. NFATC2 is a novel therapeutic target for colorectal cancer stem cells. Onco Targets Ther 2018 Oct 15;11:6911-24.
[29] Baldauf MC, Gerke JS, Orth MF, et al. Are EWSR1-NFATc2-positive sarcomas really Ewing sarcomas? Mod Pathol 2018 Jun;31(6):997-9.
[30] Berghuis D, de Hooge AS, Santos SJ, et al. Reduced human leukocyte antigen expression in advanced-stage Ewing sarcoma: implications for immune recognition. J Pathol 2009 Jun;218(2):222-31.
[31] Çelik H, Sciandra M, Flashner B, et al. Clofarabine inhibits Ewing sarcoma growth through a novel molecular mechanism involving direct binding to CD99. Oncogene 2018 Apr;37(16):2181-96.
[32] May WA, Grigoryan RS, Keshelava N, et al. Characterization and drug resistance patterns of Ewing's sarcoma family tumor cell lines. PLoS One 2013 Dec 2;8(12):e80060.
[33] Sjöblom B, Salmazo A, Djinović-Carugo K. Alpha-actinin structure and regulation. Cell Mol Life Sci 2008 Sep;65(17):2688-701.
[34] Fleuren ED, Roeffen MH, Leenders WP, et al. Expression and clinical relevance of MET and ALK in Ewing sarcomas. Int J Cancer 2013 Jul 15;133(2):427-36.
[35] Zhao SC, Zhou BW, Luo F, Mao X, Lu YJ. The structure and function of NKAIN2-a candidate tumor suppressor. Int J Clin Exp Med 2015 Oct 15;8(10):17072-9.
[36] Hanna JA, Garcia MR, Lardennois A, et al. PAX3-FOXO1 drives miR-486-5p and represses miR-221 contributing to pathogenesis of alveolar rhabdomyosarcoma. Oncogene 2018 Apr;37(15):1991-2007.
[37] Wang GY, Thomas DG, Davis JL, Ng T, Patel RM, Harms PW, Betz BL, Schuetze SM, McHugh JB, Horvai AE, Cho SJ, Lucas DR.EWSR1-NFATC2 Translocation-associated Sarcoma Clinicopathologic Findings in a Rare Aggressive Primary Bone or Soft Tissue Tumor. Am J Surg Pathol. 2019 Apr 15. https://doi.org/10.1097/PAS.0000000000001260.